BIFURCATION ANALYSIS, CLASSIFICATION OF TRAVELING WAVE SOLUTIONS, AND PERTURBATION-INDUCED CHAOTIC BEHAVIORS OF THE EXTENDED (3+1)-DIMENSIONAL NONLINEAR KUDRYASHOV'S EQUATION

Qiuyue Lin

School of Science, Jimei University
No. 185 Yinjiang Road, Jimei District, Xiamen, 361021, China
202321392022@jmu.edu.cn

Received 8 September 2025, accepted 18 November 2025, published online 7 January 2026

This paper conducts bifurcation analysis of the extended (3+1)-dimensional nonlinear Kudryashov's equation (EKE), classifies traveling wave solutions, and investigates the chaotic behaviors of the equations under specific perturbations. Firstly, the traveling wave transformation is introduced to reduce the EKE to a dynamical system, and then Gaussian solitons are obtained using the generalized trial equation method. In the following step, the existence of periodic and soliton solutions is confirmed through qualitative analysis provided by bifurcation theory and phase diagrams. To verify the conclusions of the qualitative analysis, the complete discrimination system for the polynomial method (CDSPM) is employed for classification, thus enabling the traveling wave solutions. Finally, sinusoidal and Gaussian perturbations are introduced, and the corresponding Lyapunov exponents are used to verify the existence of chaotic behaviors. This paper presents the first application of the CDSPM method to the EKE, yielding several novel results including Gaussian soliton solutions, prior estimates for periodic and soliton solutions. Additionally, traveling wave solutions in the form of hyper-elliptic functions and inverse trigonometric functions are also initially given. Finally, the chaotic behavior of the EKE under perturbation terms is presented.

DOI:10.5506/APhysPolB.57.1-A2

1. Introduction

The nonlinear Schrödinger equation (NLSE) is a widely employed mathematical model for describing nonlinear phenomena in physics [1–4]. For

instance, in condensed matter physics, it can be used to simulate macroscopic superfluid behavior in Bose–Einstein condensates [5, 6]. In nonlinear optics, the NLSE is extensively employed to describe the propagation of laser pulses through nonlinear dispersive media and the associated nonlinear wave phenomena [7, 8]. Given the significance of the NLSE, researchers have employed various methods to derive exact solutions. Ling *et al.* [9] use a unified Darboux transformation combined with a matrix analysis method to find solutions such as breathers and dark–dark solitons for the mixed coupled nonlinear Schrödinger equations under non-zero background conditions. Yıldırım *et al.* [10] employ the Lie symmetry analysis to obtain exponential-form solutions for the N-coupled NLSEs. Akhmediev *et al.* [11] use a modified Darboux transformation to derive a complete hierarchy of rational solutions for the self-focusing NLSE, revealing its connection to rogue waves. Polyanin *et al.* [12] combined the method of generalized separation of variables with the method of functional constraints to obtain traveling wave and periodic solutions for the NLSE with constant and variable delay. Kudryashov *et al.* [13] focus on the third-order derivative NLSE in the Kaup–Newell hierarchy, which is simplified by traveling wave transformation. After verifying its integrability with the Painlevé test, they derive periodic and solitary wave solutions, providing key references for higher-order NLSE dynamical analysis. These studies have significantly enhanced the theoretical understanding of nonlinear wave dynamics through innovative mathematical methods for obtaining exact solutions to the NLSE, providing a solid foundation for practical applications in fields such as optics, plasma physics, and extreme wave phenomena.

Kudryashov's equation (KE) is an important extended form of the NLSE. By introducing generalized power-law nonlinear terms, it significantly improves the accuracy of modeling wave propagation in complex optical media [14]. To further expand its application scenarios, researchers have made multiple improvements to the equation. For instance, they have introduced truncated M-fractional derivatives [15], magneto-optic parameters [16], and expanded the order of nonlinear terms [17, 18]. Besides these, Mirzazadeh *et al.* [19] have proposed the extended (3+1)-dimensional nonlinear conformable Kudryashov's equation, which generalizes the NLSE to (3+1)-dimension for the first time. Combining the flexibility and accuracy of the conformable derivative, it effectively enriches the equation's ability to describe key physical phenomena such as the memory effect of fiber pulses and 3D optical fields. It also provides important theoretical support for the design of optical devices and the optimization of optical communication systems [19]. This paper focuses on the (3+1)-dimensional extended

Kudryashov's equation (EKE). Its specific form is as follows:

$$\begin{aligned} &iq_t - (a_1 q_{xx} + a_2 q_{yy} + a_3 q_{zz} + 2a_4 q_{xy} - 2a_5 q_{xz} - 2a_6 q_{yz}) \\ &+ \left(\frac{b_1}{|q|^{2n}} + \frac{b_2}{|q|^n} + b_3 |q|^n + b_4 |q|^{2n} \right) q = 0 \,, \end{aligned} \tag{1}$$

where $q(x, y, z, t)$ is a complex waveform function, the variables x, y, z are three-dimensional spatial coordinates, and t is the time variable. a_i and b_j ($i = 1, \ldots, 6$ and $j = 1, \ldots, 4$) are the parameters for the linear and nonlinear terms, respectively.

Recently, many researchers have conducted studies on the solution of EKE exact solutions. Ur Rehman *et al.* [20] obtain exact solutions of the EKE using the ϕ^6-model expansion method. These solutions include Jacobi elliptic functions, as well as hyperbolic function solutions and trigonometric function solutions derived when a key parameter (related to the periodicity of Jacobi elliptic functions) approaches 1 or 0, such as dark solitons and bright solitons. Building on this work, Rabie *et al.* [21] adopt the extended F-expansion technique. They supplement exponential solutions and rational solutions, and analyze the influence of the specific parameter on typical dark solitons and singular solitons. Subsequently, Rabie *et al.* [22] further introduce the conformable fractional derivative. By using the improved modified extended tanh-function method, they obtain fractional-order singular periodic solutions and bright solitons, which extends the application scope to the scenario of generalized anti-cubic nonlinearity, filling the gap in fractional-order solutions of the EKE.

Although the aforementioned studies have achieved remarkable results, the solution to the traveling wave solutions of EKE remains incomplete, and the qualitative analysis is also needed. The CDSPM serves as a powerful tool to address this gap. Upon transforming the original equation into its integral form, it can construct all single traveling wave solutions of nonlinear equations [23–27]. Moreover, by systematically analyzing the structure of polynomial roots and the relationships between their coefficients, CDSPM also provides support for qualitative analysis [28, 29]. For instance, Kai *et al.* [30] apply CDSPM to the study of Ito-type coupled nonlinear wave equations, clarifying the existing conditions of solutions, revealing the system's topological properties, and providing guidance for constructing exact solutions. He *et al.* [31] also apply CDSPM to the (1+1)-dimensional Kudryashov's equation with third-order dispersion, deriving all its exact traveling wave solutions and verifying periodic and soliton solutions.

This paper uses CDSPM to carry out a thorough analysis of the EKE and derive all possible traveling wave solutions. Section 2 transforms EKE into a traveling wave system and uses the generalized trial method to derive

Gaussian soliton solutions under specific parameter conditions. Section 3 performs a qualitative analysis of the resulting dynamical system to confirm the existence of periodic and soliton solutions using the bifurcation theory and phase diagrams. Section 4 classifies and solves all exact traveling wave solutions using CDSPM, thereby verifying the aforementioned qualitative conclusions. Section 5 introduces specific perturbation terms and uses the Lyapunov exponents to explore chaotic behaviors. Section 6 summarizes the paper.

2. Reduced system under traveling wave transformation

In this section, we introduce the following transformation to simplify EKE into a traveling wave system:

$$\begin{aligned} u(x,y,z,t) &= W(\eta)\,\mathrm{e}^{i\Psi(x,y,z,t)}\,, \\ \Psi(x,y,z,t) &= -p_1x - p_2y - p_3z + \Omega t + \phi_0\,, \\ \eta &= Q_1x + Q_2y + Q_3z - st\,, \end{aligned} \tag{2}$$

where $Q_1,\ Q_2,\ Q_3$ are the spatial direction weights, $p_1,\ p_2,\ p_3$ are the wave numbers in each direction, s is the wave velocity, Ω is the angular frequency, and ϕ_0 is the initial phase constant.

Substituting Eq. (2) into Eq. (1) and separating the imaginary and real parts, the imaginary and real parts are obtained as follows:

$$\begin{aligned} s &= 2Q_1(\alpha_1p_1 + \alpha_4p_2 - \alpha_5p_3) + 2Q_2(\alpha_2p_2 + \alpha_4p_1 - \alpha_6p_3) \\ &\quad +2Q_3(\alpha_3p_3 - \alpha_5p_1 - \alpha_6p_2)\,, \end{aligned} \tag{3}$$

and

$$-MW'' + (-\Omega + N)W + b_1W^{1-2n} + b_2W^{1-n} + b_3W^{1+n} + b_4W^{1+2n} = 0\,, \tag{4}$$

where

$$M = a_1Q_1^2 + a_2Q_2^2 + a_3Q_3^2 - 2a_4Q_1Q_2 - 2a_5Q_1Q_3 - 2a_6Q_2Q_3\,, \tag{5}$$

and

$$N = a_1p_1^2 + a_2p_2^2 + a_3p_3^2 + 2a_4p_1p_2 - 2a_5p_1p_3 - 2a_6p_2p_3\,. \tag{6}$$

In order to simplify Eq. (4), we introduce the following transformation:

$$W = Z^{1/n}\,, \tag{7}$$

then we get

$$\begin{aligned} &-nMZZ'' - M(1-n)\left(Z'\right)^2 + n^2b_1 + n^2b_2Z + n^2(-\Omega + N)Z^2 \\ &+n^2b_3Z^3 + n^2b_4Z^4 = 0\,. \end{aligned} \tag{8}$$

Regarded this, we have

$$h_5 Z Z'' + h_6 \left(Z'\right)^2 = h_0 + h_1 Z + h_2 Z^2 + h_3 Z^3 + h_4 Z^4 \,, \tag{9}$$

where

$$\begin{aligned} h_0 &= n^2 b_1 \,, \qquad h_1 = n^2 b_2 \,, \qquad h_2 = n^2(-\Omega + N) \,, \\ h_3 &= n^2 b_3 \,, \qquad h_4 = n^2 b_4 \,, \qquad h_5 = -nM \,, \qquad h_6 = -M(1-n) \,. \end{aligned} \tag{10}$$

If $h_5 \neq 0$, Eq. (9) can be rewritten as

$$Z'' - f_1 \left(Z'\right)^2 = Z F(Z) \,, \tag{11}$$

where

$$f_1 = \frac{1-n}{n} \,, \qquad F(Z) = m_0 Z^{-1} + m_1 Z + m_2 Z^2 + m_3 Z^3 + m_4 \tag{12}$$

with coefficients

$$m_0 = b_1 \,, \qquad m_1 = N - \Omega \,, \qquad m_2 = b_3 \,, \qquad m_3 = b_4 \,, \qquad m_4 = b_2 \,. \tag{13}$$

Gaussian solitons, as a special type of localized solution, hold significant physical importance in nonlinear optics and wave propagation [32]. If the parameters in Eq. (9) satisfy the following conditions:

$$h_0 = h_1 = h_3 = h_4 = 0 \,, \qquad h_2 = -2 \,, \qquad h_5 = 1 \,, \qquad h_6 = -1 \,, \tag{14}$$

then transform Eq. (9) into

$$Z Z'' - \left(Z'\right)^2 + 2Z^2 = 0 \,. \tag{15}$$

Next, we employ the generalized trial method [33], and the corresponding Gaussian soliton solution can be obtained as

$$Z(\eta) = D \, \mathrm{e}^{-(\eta - \eta_0)^2} \,, \tag{16}$$

as shown in Fig. 1.

In this section, the EKE is simplified to a traveling wave system. Building on this, the section presents the Gaussian soliton solution to the EKE for the first time, obtained via the generalized trial method, and provides its corresponding graphical representation.

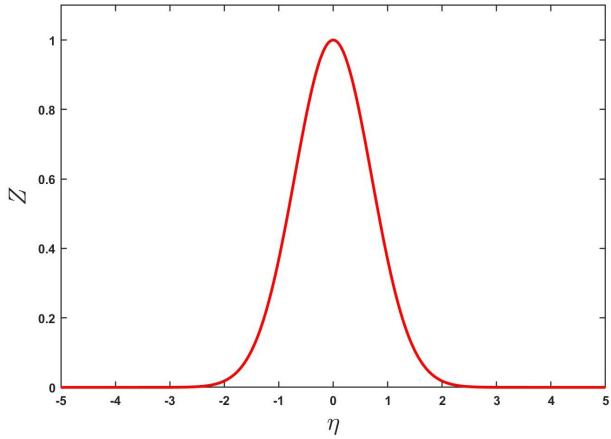

Fig. 1. The Gaussian soliton solution. The case of $D = 1,\ \eta_0 = 0$ in Eq. (16).

3. Qualitative analysis

In this section, the focus remains on the traveling wave system, Eq. (11), that was introduced in the preceding section.

In order to focus on key dynamical behaviors, such as equilibrium points, we first transform Eq. (11) into the following two-dimensional dynamical system form:

$$\begin{cases} \rho = Z\,, \\ Z' = F(Z) + \dfrac{f_1}{Z}\rho^2\,. \end{cases} \tag{17}$$

Using the first integral method, we obtain

$$\left(Z'\right)^2 = r_0 + r_1 Z + r_2 Z^2 + r_3 Z^3 + r_4 Z^4 + r_5 Z^{2f_1}\,, \tag{18}$$

where

$$\begin{aligned} r_0 &= -\frac{2}{5}b_1\,, \qquad r_1 = -\frac{1}{2}b_2\,, \qquad r_2 = -\frac{2}{3}(N-\Omega)\,, \\ r_4 &= -2b_4\,, \qquad r_5 = C\,, \end{aligned} \tag{19}$$

and C is a constant of integration.

Considering that the integral form derived from Eq. (18) is usually impossible to solve precisely, we take $f_1 = \frac{5}{2}$ as an example for discussion. It should be noted that when f_1 takes different values, this method can be applied in a similar manner. When $f_1 = \frac{5}{2}$, Eq. (18) can be written as

$$\left(Z'\right)^2 = r_0 + r_1 Z + r_2 Z^2 + r_3 Z^3 + r_4 Z^4 + r_5 Z^5\,. \tag{20}$$

We introduce the transformation

$$Z = \phi - \frac{r_4}{5r_5}\,, \tag{21}$$

then we get

$$\left(\phi'\right)^2 = k_5\phi^5 + k_3\phi^3 + k_2\phi^2 + k_1\phi + k_0\,. \tag{22}$$

Next, we transform Eq. (22) into the following dynamical system:

$$\begin{cases} \phi = \upsilon\,, \\ \upsilon' = \dfrac{5}{2}k_5\phi^4 + \dfrac{3}{2}k_3\phi^2 + k_2\phi + k_1\,. \end{cases} \tag{23}$$

The corresponding Hamiltonian can be written as

$$H(\upsilon,\phi) = \frac{1}{2}\upsilon^2 - \frac{1}{2}\left(k_5\phi^5 + k_3\phi^3 + k_2\phi^2 + k_1\phi\right)\,, \tag{24}$$

which satisfies

$$\frac{\partial H}{\partial \phi} = \upsilon'\,, \qquad \frac{\partial H}{\partial \upsilon} = -\phi'\,. \tag{25}$$

To introduce the properties of equilibrium points, we introduce the derivative of the negative potential energy function as follows:

$$-U'(\phi) = \frac{5}{2}k_5\left(\phi^4 + s_2\phi^2 + s_1\phi + s_0\right)\,, \tag{26}$$

where

$$s_0 = \frac{k_1}{5k_5}\,, \qquad s_1 = \frac{2k_2}{5k_5}\,, \qquad s_2 = \frac{3k_3}{5k_5}\,. \tag{27}$$

Since Eq. (23) is an autonomous system, its trajectory corresponds to the contour lines of the Hamiltonian. To investigate the properties of equilibrium points in the dynamical system, the relationship between the roots and coefficients is analyzed. We introduce the following complete discriminant system of the fourth order:

$$\begin{aligned} O_2 &= 9s_2^2 - 32s_2s_0\,, \qquad K_1 = 4\,, \qquad K_2 = -s_2\,, \\ K_3 &= -s_2^3 + 8s_2s_0 - 9s_1^2\,, \\ K_4 &= -s_2^3s_1^2 + 4s_2^4s_0 + 36s_2s_1^2 - 32s_2^2s_0^2 - \frac{27}{4}s_1^4 + 64s_0^3\,. \end{aligned} \tag{28}$$

According to the complete discriminant system, the quartic polynomial can be classified into nine categories. Two of these are rarely observed in physical applications, so below we focus on the seven representative types.

Type I

$K_4 > 0$, $K_3 > 0$, $K_2 > 0$,

$$-U'(\phi) = \frac{5}{2}k_5(\phi-\alpha)(\phi-\beta)(\phi-\gamma)(\varphi-\delta)\,,$$
$$(\alpha+\beta+\gamma+\delta = 0\,, \quad \alpha<\beta<\gamma<\delta)\,. \tag{29}$$

In this case, the system has four equilibrium points: $(\alpha,0)$, $(\beta,0)$, $(\gamma,0)$, and $(\delta,0)$. When $k_5 > 0$, $(\alpha,0)$ and $(\gamma,0)$ are saddle points, and $(\beta,0)$ and $(\delta,0)$ are center points. When $k_5 < 0$, $(\alpha,0)$ and $(\gamma,0)$ are center points, and $(\beta,0)$ and $(\delta,0)$ are saddle points. If we take $k_5 = \pm 1$, $k_3 = \pm\frac{40}{3}$, $k_2 = 0$, and $k_1 = \pm 5$, we obtain $\alpha = -3$, $\beta = -1$, $\gamma = 1$, and $\delta = 3$. The corresponding phase diagram is shown in Fig. 2. In Fig. 2 (a), the red closed trajectory surrounding the center corresponds to a periodic solution, while the blue homoclinic trajectory passing through the saddle point indicates the existence of a bell-shaped soliton solution. Similarly, in Fig. 2 (b), the red trajectory corresponds to a periodic solution, and the blue trajectory corresponds to a bell-shaped soliton solution.

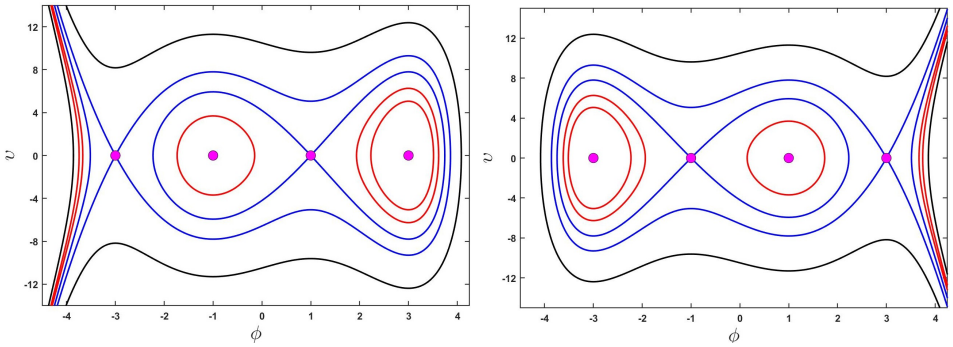

(a) (b)

Fig. 2. Type I: Phase diagram of Eq. (29): (a) $k_5 = 1$; (b) $k_5 = -1$.

Type II

$K_3 = K_4 = 0$, $O_2 > 0$, $K_2 < 0$,

$$-U'(\phi) = \frac{5}{2}k_5(\phi-\alpha)^3(\phi-\beta), \qquad (3\alpha+\beta = 0\,, \quad \alpha<\beta)\,. \tag{30}$$

In this case, the system has two equilibrium points, $(\alpha,0)$, and $(\beta,0)$. When $k_5 > 0$, $(\alpha,0)$ is a cuspidal point and $(\beta,0)$ is a center point. When $k_5 < 0$, $(\alpha,0)$ is a center point and $(\beta,0)$ is a saddle point. If $k_5 = \pm 1$, $k_3 = 0$,

$k_2 = \pm\frac{5}{4}$, and $k_1 = \pm\frac{5}{16}$, then $\alpha = -0.5$ and $\beta = 1.5$. The corresponding image diagram is shown in Fig. 3. In Fig. 3 (a), the red trajectory lines indicate the existence of periodic solutions. Similarly, in Fig. 3 (b), the red trajectory lines indicate the existence of periodic solutions, while the blue trajectory lines indicate the existence of bell-shaped soliton solutions.

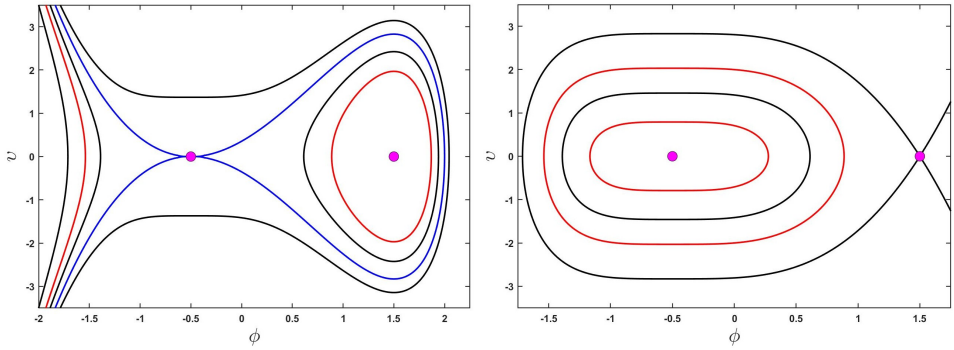

(a) (b)

Fig. 3. Type II: Phase diagram of Eq. (30): (a) $k_5 = 1$; (b) $k_5 = -1$.

Type III

$K_4 = 0$, $K_3 \neq 0$, $K_2 > 0$,

$$-U'(\phi) = \tfrac{5}{2} r_5 (\phi - \alpha)^2 (\phi - \beta)(\phi - \gamma)\,,$$
$$(2\alpha + \beta + \gamma = 0\,, \quad \gamma < \alpha < \beta)\,. \tag{31}$$

In this case, the system has three equilibrium points: $(\alpha, 0)$, $(\beta, 0)$, and $(\gamma, 0)$. When $k_5 > 0$, $(\alpha, 0)$ is a cuspidal point, $(\beta, 0)$ is a saddle point, and $(\gamma, 0)$ is a center point. When $k_5 < 0$, $(\alpha, 0)$ is a cuspidal point, $(\beta, 0)$ is a center point, and $(\gamma, 0)$ is a saddle point. If $k_5 = \pm 1$, $k_3 = \pm\frac{5}{3}$, $k_2 = k_1 = 0$, then $\alpha = 0$, $\beta = 1$, and $\gamma = -1$. The corresponding phase diagram is shown in Fig. 4. In Fig. 4 (a), the red trajectory indicates the existence of periodic solutions, while the blue trajectory, which starts from the cuspidal point and returns to the same cuspidal point, is a homoclinic orbit, indicating the existence of bell-shaped soliton solutions. Similarly, the red trajectory in Fig. 4 (b) indicates the existence of periodic solutions, and the blue trajectory indicates the existence of bell-shaped soliton solutions.

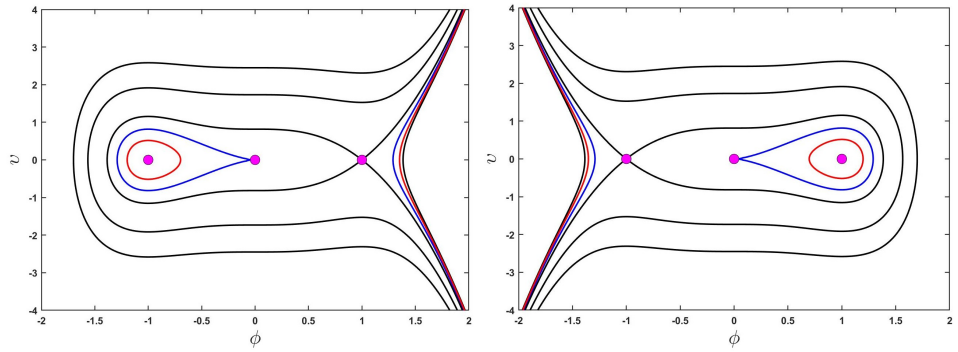

(a) (b)

Fig. 4. Type III: Phase diagram of Eq. (31): (a) $k_5 = 1$; (b) $k_5 = -1$.

Type IV

$K_4 < 0$, $K_2 K_3 \geq 0$,

$$-U'(\phi) = \frac{5}{2} k_5 \left[(\phi - \alpha)^2 + \beta^2\right](\phi - \gamma)(\phi - \delta)\,,$$
$$(2\alpha + \gamma + \delta = 0\,, \quad \gamma > \delta)\,. \tag{32}$$

In this case, the system has two equilibrium points, $(\gamma, 0)$ and $(\delta, 0)$. When $k_5 > 0$, $(\delta, 0)$ is a saddle point and $(\gamma, 0)$ is a center point. When $k_5 < 0$, $(\delta, 0)$ is the center point, and $(\gamma, 0)$ is the saddle point. If we set $k_1 = \pm 1$, $k_3 = \pm 5$, $k_2 = 0$, and $k_1 = \pm 20$, we obtain $\alpha = 0$, $\beta = 1$, $\gamma = 2$, and $\delta = -2$. The corresponding phase diagram is shown in Fig. 5, where the red trajectory indicates the existence of periodic solutions, and the blue trajectory indicates the existence of bell-shaped soliton solutions.

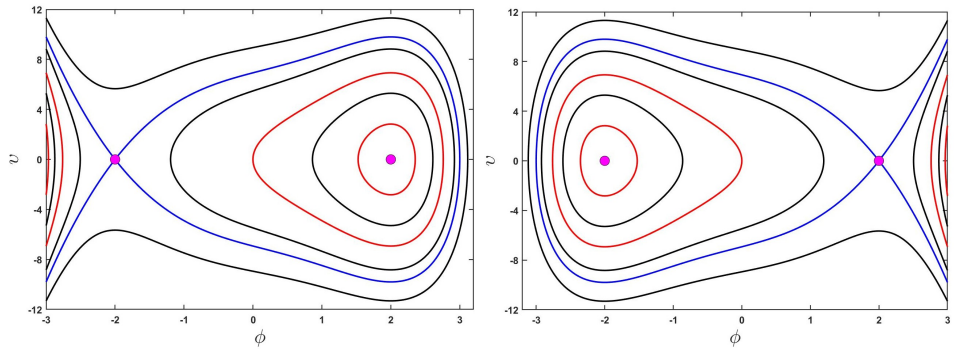

(a) (b)

Fig. 5. Type IV: Phase diagram of Eq. (32): (a) $k_5 = 1$; (b) $k_5 = -1$.

The following discussion addresses the special case, where the equilibrium point is the sole type of cuspidal points. As this represents solutions for a finite class only, this paper shall treat it succinctly.

Type V

$K_3 = K_4 = 0,\ K_2 \leq 0,\ s_2 = s_1 = s_0 = 0,$

$$-U'(\phi) = \frac{5}{2} r_5 \phi^4 \,. \tag{33}$$

In this case, the system has a unique equilibrium point $(0, 0)$, which is a cuspidal point. When $k_5 > 0$ and $k_5 < 0$, the behavior of the system is the same.

Type VI

$K_2 K_3 < 0,\ K_4 = 0,$

$$\begin{aligned} -U'(\phi) &= \frac{5}{2} k_5 (\phi - \alpha)^2 \left[(\phi - \beta)^2 + \gamma^2 \right] , \\ (\alpha + \beta &= 0) \,. \end{aligned} \tag{34}$$

The system has a unique equilibrium point $(\alpha, 0)$, which is a cuspidal point. For $k_5 > 0$ and $k_5 < 0$, the behavior is the same. Similar to type V.

Type VII

$K_4 = K_3 = O_2 = 0,\ K_2 > 0,$

$$\begin{aligned} -U'(\phi) &= \frac{5}{2} r_5 (\phi - \alpha)^2 (\phi - \beta)^2 \,, \\ (\alpha + \beta &= 0) \,. \end{aligned} \tag{35}$$

In this case, there are two equilibrium points, $(\alpha, 0)$ and $(\beta, 0)$. When $k_5 > 0$, both points are cuspidal points, and when $k_5 < 0$, they remain cuspidal points. This case can be interpreted as a double cuspidal point extension of the single cuspidal point case shown in type V.

This section formulates the Hamiltonian according to the traveling wave system. Employing CDSPM to examine the relationship between the polynomial roots and coefficients of the potential energy function, we determine the type of equilibrium points and corresponding trajectories through bifurcation analysis, thereby proving the existence of periodic and soliton solutions. In the subsequent section, all traveling wave solutions will be presented to substantiate the conclusions drawn in this part.

4. Precise wave solutions

This section studies the exact traveling wave solutions for Eq. (22) to support the qualitative insights from Section 3. Letting $k_5 = 1$ (other value of k_5 could be trained similarly), Eq. (22) transforms into

$$\left(\phi'\right)^2 = \phi^5 + k_3\phi^3 + k_2\phi^2 + k_1\phi + k_0\,. \tag{36}$$

The integral representation is

$$\pm(\eta - \eta_0) = \int \frac{\mathrm{d}\phi}{\sqrt{\phi^5 + k_3\phi^3 + k_2\phi^2 + k_1\phi + k_0}}\,, \tag{37}$$

where η_0 serves as a constant of integration.

We define a polynomial as

$$R(\phi) = \phi^5 + k_3\phi^3 + k_2\phi^2 + k_1\phi + k_0\,. \tag{38}$$

To systematically classify root structures and provide integral forms for subsequent solutions, we now introduce the complete discriminant system for Eq. (38)

$$\begin{aligned}
O_2 &= 3k_2^2 - 8k_1k_3\,, \qquad K_2 = -k_3\,,\\
K_3 &= 40k_3k_1 - 12k_3^3 - 45k_2^2\,,\\
K_4 &= 12k_4^3k_1 - 4k_3^3k_2^2 + 117k_3k_1k_2^2 - 88k_1^2k_2^3\\
&\quad -40k_2k_0k_2^3 - 27k_4^2 - 300k_2k_1k_0 + 160k_1^3\,,\\
K_5 &= -1600k_2k_0k_1^3 - 3750k_2k_3k_0^3 + 2000k_3k_1^2k_0^2\\
&\quad -4k_3^3k_2^2k_1^2 + 16k_3^3k_2^3k_0 - 900k_1k_0^2k_3^3\\
&\quad +825k_3^2k_2^2k_0^2 + 144k_3k_2^2k_1^3 + 16k_3^4k_1^3\\
&\quad +108k_5^3k_2^0 - 128k_1^4k_3^2 - 27k_1^2k_2^4 + 3125k_0^4\\
&\quad +108k_0k_2^5 + 2250k_1k_2^2k_0^2 - 72k_2k_1k_0k_3^4\\
&\quad +560k_0k_2k_1^2k_3^2 - 630k_0k_1k_3k_2^3\,,\\
J_2 &= 160k_1^2k_3^2 + 900k_2^2k_1^2 - 48k_1k_3^5 + 60k_1k_2^2k_3^2\\
&\quad +16k_2^2k_3^4 + 1500k_3k_2k_1k_0 + 625k_0^2k_3^2\\
&\quad -1100k_3^3k_0k_2 - 3375k_0k_2^3\,.
\end{aligned} \tag{39}$$

Based on the above system, we explore 12 cases for the traveling wave solutions of Eq. (38).

Case (1)

When $K_4 = K_5 = 0$, $K_3 > 0$, $J_2 \neq 0$, $R(\phi)$ can be expressed as follows:

$$R(\phi) = (\phi - u_1)^2(\phi - u_2)^2(\phi - u_3)\,. \tag{40}$$

Assuming $\phi > u_3$, we obtain the following solutions:

1. if $u_3 > u_1$, $u_3 > u_2$, we get

$$\begin{aligned}\pm(u_1 - u_2)(\eta - \eta_0) \;=\; & 2\sqrt{u_3 - u_1}\arctan\sqrt{\frac{\phi - u_3}{u_3 - u_1}} \\ & -2\sqrt{u_3 - u_2}\arctan\sqrt{\frac{\phi - u_3}{u_3 - u_2}}\,;\end{aligned} \tag{41}$$

2. if $u_3 < u_2$, $u_3 > u_1$, we obtain

$$\begin{aligned}\pm(u_1 - u_2)(\eta - \eta_0) \;=\; & 2\sqrt{u_3 - u_1}\arctan\sqrt{\frac{\phi - u_3}{u_3 - u_1}} \\ & -\frac{2}{\sqrt{u_2 - u_3}}\ln\left|\frac{\sqrt{\phi - u_3} - \sqrt{u_2 - u_3}}{\sqrt{\phi - u_3} + \sqrt{u_2 - u_3}}\right|\,;\end{aligned} \tag{42}$$

3. if $u_3 < u_1$, $u_3 > u_2$, we get

$$\begin{aligned}\pm(u_1 - u_2)(\eta - \eta_0) \;=\; & \frac{1}{\sqrt{u_1 - u_3}}\ln\left|\frac{\sqrt{\phi - u_3} - \sqrt{u_1 - u_3}}{\sqrt{\phi - u_3} + \sqrt{u_1 - u_3}}\right| \\ & -2\sqrt{u_3 - u_1}\arctan\sqrt{\frac{\phi - u_3}{u_3 - u_2}}\,.\end{aligned} \tag{43}$$

When $u_1 = 2$, $u_2 = -0.1$, $u_3 = 1.3$, $\eta_0 = 0$, as shown in Fig. 6, a dark soliton appears.

4. if $u_3 < u_1$, $u_3 < u_2$, the corresponding solution is expressed as follows:

$$\begin{aligned}\pm(u_1 - u_2)(\eta - \eta_0) \;=\; & \frac{1}{\sqrt{u_1 - u_3}}\ln\left|\frac{\sqrt{\phi - u_3} - \sqrt{u_1 - u_3}}{\sqrt{\phi - u_3} + \sqrt{u_1 - u_3}}\right| \\ & -\frac{1}{\sqrt{u_2 - u_3}}\ln\left|\frac{\sqrt{\phi - u_3} - \sqrt{u_2 - u_3}}{\sqrt{\phi - u_3} + \sqrt{u_2 - u_3}}\right|\,.\end{aligned} \tag{44}$$

When $u_1 = 7$, $u_2 = 5$, $u_3 = 1.3$, $\eta_0 = 0$, as demonstrated in Fig. 7, a singular soliton solution is evident.

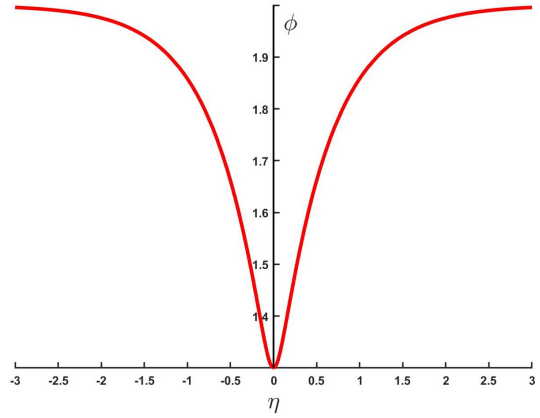

Fig. 6. The graphical representation of dark soliton solution.

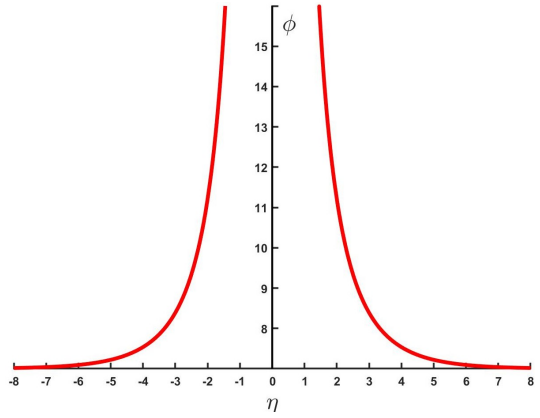

Fig. 7. The graphical representation of singular soliton solution.

Case (2)

When $K_3 = K_4 = K_5 = O_2 = 0$, $K_2 \neq 0$, $R(\phi)$ can be given as follows:

$$R(\phi) = (\phi - u_1)^4(\phi - u_2)\,. \tag{45}$$

Assuming $\phi > u_2$, we obtain the following solution:

1. if $u_1 > u_2$, we obtained the following solution:

$$\pm(u_2-u_1)(\eta-\eta_0) = \frac{1}{\sqrt{\phi-u_2}}+\frac{1}{2\sqrt{u_1-u_2}}\ln\left|\frac{\sqrt{\phi-u_2}-\sqrt{u_1-u_2}}{\sqrt{\phi-u_2}+\sqrt{u_1-u_2}}\right|\,; \tag{46}$$

2. if $u_2 > u_1$, we get

$$\pm(u_2-u_1)(\eta-\eta_0) = \frac{\sqrt{\phi-u_2}}{\phi-u_1}+\frac{1}{\sqrt{u_2-u_1}}\arctan\sqrt{\frac{\phi-u_2}{u_2-u_1}}\,. \tag{47}$$

Case (3)

When $K_3 = K_4 = K_5 = 0$, $K_2 \neq 0$, $O_2 \neq 0$, $R(\phi)$ can be written as

$$R(\phi) = (\phi - u_1)^3(\phi - u_2)^2 \,. \tag{48}$$

Assuming $\phi > u_1$, we obtain the following solution:
1. if $u_2 > u_1$, we get

$$\pm(u_2 - u_1)(\eta - \eta_0) = \frac{1}{\phi - u_1} + \sqrt{u_1 - u_2}\arctan\sqrt{\frac{\phi - u_1}{u_2 - u_2}}\,; \tag{49}$$

2. if $u_1 > u_2$, we obtain

$$\pm(u_2 - u_1)(\eta - \eta_0) = \frac{1}{\sqrt{u_2 - u_1}}\ln\left|\frac{\sqrt{\phi - u_1} - \sqrt{u_2 - u_1}}{\sqrt{\phi - u_1} + \sqrt{u_2 - u_1}}\right| + \frac{2}{\phi - u_1}\,; \tag{50}$$

Case (4)

When $K_2 = K_3 = K_4 = K_5 = 0$, $R(\phi)$ can be given as

$$R(\phi) = (\phi - u_1)^5 \,. \tag{51}$$

For $u_1 = 0$ and $\eta_0 = 0$, corresponding solutions are $\phi_1 = \frac{3}{2}\eta^{3/2}$ and $\phi_2 = -\frac{3}{2}\eta^{-3/2}$.

Case (5)

When $K_4 = K_5 = 0$, $K_3 < 0$, $O_2 \neq 0$, $R(\phi)$ can be presented in the following form:

$$R(\phi) = (\phi - u_1)\left(\phi^2 + c\phi + l\right)^2 \,. \tag{52}$$

When $c^2 - 4l < 0$, we get

$$\begin{aligned}\pm(\eta - \eta_0) \;=\; & -\frac{2}{\lambda\sqrt{4l - c^2}}\cos\xi\arctan\left(\frac{2\lambda\sin\xi\sqrt{\phi - u_1}}{\phi - u_1}\right) \\ & +\frac{\sin\xi}{2}\ln\left(\frac{\phi - u_1 - \lambda^2 - 2\lambda\cos\xi\sqrt{\phi - u_1}}{\phi - u_1 - \lambda^2 + 2\lambda\cos\xi\sqrt{\phi - u_1}}\right)\,,\end{aligned} \tag{53}$$

where

$$\lambda = (u_1^2 + cu_1 + l)^{\frac{1}{4}}\,, \qquad \xi = \frac{1}{2}\arctan\sqrt{\frac{4l - c^2}{-2u_1 - c}}\,. \tag{54}$$

For the subsequent Cases (6)–(9), the roots of the polynomial involve higher multiplicities or combinations, rendering it impossible to obtain closed-form expressions using elementary functions alone. In such instances, elliptic

integrals prove indispensable for deriving exact solutions, providing rigorous representations for periodic waves [34]. Therefore, we introduce the following elliptic integral:

$$\begin{aligned} W(\varphi,\kappa) &= \int_0^{\varphi} \frac{\mathrm{d}\varphi}{\sqrt{1-\kappa^2\sin^2\varphi}}, \\ L(\varphi,q,\kappa) &= \int_0^{\varphi} \frac{\mathrm{d}\varphi}{\left(1+q\sin^2\varphi\right)\sqrt{1-\kappa^2\sin^2\varphi}}, \\ G(\varphi,\kappa) &= \int_0^{\varphi} \sqrt{1-\kappa^2\sin^2\varphi}\,\mathrm{d}\varphi. \end{aligned} \tag{55}$$

Case(6)

When $K_4 = K_5 = O_2 = 0$, $K_3 > 0$, $R(\phi)$ can be expressed as

$$R(\phi) = (\phi-u_1)^3(\phi-u_2)(\phi-u_3). \tag{56}$$

We have the following three classifications:

1. if $u_1 > u_2 > u_3$, we have obtained the following solution:

$$\begin{aligned} \pm(u_2-u_1)(\eta-\eta_0) &= \frac{2\sqrt{\phi-u_2}}{\sqrt{(\phi-u_3)(\phi-u_1)}} \\ &\quad -\frac{2}{\sqrt{u_1-u_3}}G\left(\arcsin\sqrt{\frac{u_1-u_3}{\phi-u_3}}, \frac{\sqrt{u_2-u_3}}{\sqrt{u_1-u_3}}\right); \end{aligned} \tag{57}$$

2. if $u_2 > u_1 > u_3$, we get

$$\begin{aligned} \pm(u_2-u_1)(\eta-\eta_0) &= \frac{2}{\sqrt{u_1-u_3}}G\left(\arcsin\sqrt{\frac{u_1-u_3}{\phi-u_3}}, \sqrt{\frac{u_2-u_3}{u_1-u_3}}\right) \\ &\quad -\frac{2\sqrt{\phi-u_2}}{\sqrt{(\phi-u_1)(\phi-u_3)}}; \end{aligned} \tag{58}$$

3. if $u_1 > u_3 > u_2$, we obtain

$$\begin{aligned} \pm(u_2-u_1)(\eta-\eta_0) &= \frac{2\sqrt{\phi-u_2}}{\sqrt{(\phi-u_1)(\phi-u_3)}} \\ &\quad -\frac{2}{\sqrt{u_1-u_3}}G\left(\arcsin\sqrt{\frac{u_1-u_3}{\phi-u_3}}, \sqrt{\frac{u_3-u_2}{u_1-u_3}}\right). \end{aligned} \tag{59}$$

Case (7)

When $K_5 = 0$, $K_4 > 0$, $R(\phi)$ can be written as

$$R(\phi) = (\phi - u_1)^2(\phi - u_2)(\phi - u_3)(\phi - u_3)(\phi - u_4)\,. \tag{60}$$

We obtain the following solution:

$$\pm(u_3 - u_1)(\eta - \eta_0) = \frac{2}{\sqrt{u_3 - u_4}}\left\{W(\varphi, \kappa) - q\,L(\varphi, q, \kappa)\right\}\,, \tag{61}$$

where

$$q = \frac{u_2 - u_3}{u_2 - u_1}\,. \tag{62}$$

It is clear that Eq. (61) is in the form of the periodic solution.

Case (8)

When $K_5 = 0$, $K_4 < 0$, $R(\phi)$ can be expressed in the following form:

$$R(\phi) = (\phi - u_1)^2(\phi - u_2)\left[(\phi - c)^2 + l^2\right]\,, \tag{63}$$

1. if $u_1 = c - l\tan\theta$, we have

$$\pm(\eta - \eta_0) = \sqrt{\frac{\sin^2 2\sigma}{4l^3}}\left[\frac{1}{\kappa}\arcsin(\kappa\sin\varphi) - W(\varphi, \kappa)\right]\,; \tag{64}$$

2. if $u_1 = c + l\cot\theta$, we get

$$\pm(\eta - \eta_0) = \sqrt{\frac{\sin^3 2\varphi}{4l^3}} \times\left(W(\varphi, \kappa) - \frac{1}{\sqrt{1 - \kappa^2}} \times \ln\frac{\sqrt{1 - \kappa^2\sin^2\varphi} + \sqrt{1 - \kappa^2}\sin\varphi}{\cos\varphi}\right)\,; \tag{65}$$

3. if $u_1 \neq c - l\tan\theta$ and $u_1 \neq c + l\cot\theta$, we obtain

$$\begin{aligned}\pm(\eta - \eta_0) \;=\; & \frac{\tan\sigma + \cot\sigma}{2(u_2\tan\sigma - c - u_1)\sqrt{\frac{u_2}{\sin^3 2\sigma}}}\,W(\varphi, \kappa) - \frac{u_2\tan\sigma + u_2\cot\sigma}{u_2\cot\sigma + c_1 + u_1} \\ & \times\left\{\frac{\tan\sigma + c + u_1}{(u_2\cot\sigma + c - u_1)\sin\varphi}\right. \\ & \left.\times\sqrt{1 - \kappa^2\sin^2\varphi} + W(\varphi, \kappa) - G(\varphi, \kappa)\right\}\,,\end{aligned} \tag{66}$$

where

$$\kappa = \sin\sigma\,, \qquad \cos 2\sigma = \frac{\kappa(u_1 - c)}{l}\,, \qquad \tan 2\sigma = \frac{l}{u_1 - c}\,, \qquad 0 < \sigma < \frac{\pi}{2}\,. \tag{67}$$

Case (9)

When $J_2 = K_4 = K_5 = 0$, $K_3 < 0$, we have

$$R(\phi) = (\phi - u_1)^3 \left[(\phi - c)^2 + l^2\right] , \tag{68}$$

1. if $u_1 = c + l$, we have obtained the following solution:

$$\pm(\eta - \eta_0) = \sqrt{\frac{\sin^3 2\sigma}{4l^3}} \left(\frac{1}{k} \arcsin(k \sin\varphi) - W(\varphi, k) \right) ; \tag{69}$$

2. if $u_1 \neq c + l$, we obtain

$$\begin{aligned} \pm(\eta - \eta_0) \; = \; & \frac{\tan\sigma + \cot\sigma}{2(l\tan\sigma - c - u_1)\sqrt{\frac{l}{\sin^3 2\sigma}}} W(\varphi, \kappa) - \frac{l\tan\sigma + l\cot\sigma}{l\cot\sigma + c + \alpha} \\ & \times \left\{ \frac{\tan\sigma + c + u_1}{(l\cot\sigma + c - u_1)\sin\varphi} \sqrt{1 - \kappa^2 \sin^2\varphi} \right. \\ & \left. + W(\varphi, \kappa) - G(\varphi, \kappa) \right\} . \end{aligned} \tag{70}$$

In the following 3 cases, we will use hyper-elliptic functions and hyper-elliptic integrals for discussion.

Case (10)

When $K_5 < 0$, we have

$$R(\phi) = (\phi - u_1)(\phi - u_2)(\phi - u_3) \left[(\phi - c)^2 + l^2\right] . \tag{71}$$

We can obtain the following solution:

$$\pm(\eta - \eta_0) = \int \frac{\mathrm{d}\phi}{\sqrt{(\phi - u_1)(\phi - u_2)(\phi - u_3)\left[(\phi - c)^2 + l^2\right]}} . \tag{72}$$

Case (11)

When $K_2 \leq 0$, $K_5 > 0$ or $K_3 \leq 0$, $K_5 > 0$ or $K_4 \leq 0$, $K_5 > 0$, $R(\phi)$ can be written as

$$R(\phi) = (\phi - u_1) \left[(\phi - c_1)^2 + l_1^2\right] \left[(\phi - c_2)^2 + l_2^2\right] . \tag{73}$$

We obtain the following solution:

$$\pm(\eta - \eta_0) = \int \frac{\mathrm{d}\phi}{\sqrt{(\phi - u_1)\left[(\phi - c_1)^2 + l_1^2\right]\left[(\phi - c_2)^2 + l_2^2\right]}} . \tag{74}$$

Case (12)

When $K_2 > 0$, $K_3 > 0$, $K_4 > 0$, $K_5 > 0$, we obtain

$$R(\phi) = (\phi - u_1)(\phi - u_2)(\phi - u_3)(\phi - u_4)(\phi - u_5)\,. \tag{75}$$

We have the following solution:

$$\pm(\eta - \eta_0) = \int \frac{\mathrm{d}\phi}{\sqrt{(\phi - u_1)(\phi - u_2)(\phi - u_3)(\phi - u_4)(\phi - u_5)}}\,. \tag{76}$$

In this section, we transform Eq. (38) into integral form and introduce the CDSPM. By classifying the relationship between roots and coefficients, we present the integral forms of traveling wave solutions for 12 cases, thereby deriving all traveling wave solutions. These solutions involve inverse trigonometric functions, logarithmic functions, and hyper-elliptic function solutions. It is noteworthy that we have initially constructed the hyper-elliptic function solution for the EKE equations. In this section, we also present examples of periodic solutions for Case (7) and provide graphical representations of the dark soliton and singular soliton solutions corresponding to Case (1), which verifies the qualitative conclusions regarding the existence of periodic waves and soliton waves discussed in Section 3.

5. Perturbation-induced chaotic behaviors

In practical physical systems such as fibre propagation modeled by nonlinear equations, external perturbations such as noise or periodic forces are unavoidable [35, 36]. Under certain parametric conditions, these perturbations can trigger transitions from stable periodic or soliton behaviors to chaotic dynamics, which is crucial for understanding wave instabilities and nonlinear effects [37].

Since Eq. (23) is an autonomous dynamical system, to investigate its chaotic behaviors, we introduce a perturbation function $\Lambda(\eta)$ into (23), yielding the following perturbed system:

$$\begin{cases} \phi = \upsilon\,, \\ \upsilon' = \dfrac{5}{2}k_5\phi^4 + \dfrac{3}{2}k_3\phi^2 + k_2\phi + \dfrac{1}{2}k_1 + \Lambda(\eta)\,, \end{cases} \tag{77}$$

where $a = \frac{5}{2}k_5$, $b = \frac{3}{2}k_3$, $c = k_2$, $d = \frac{1}{2}k_1$.

In the subsequent stage of the investigation, two distinct categories of perturbation terms are introduced.

Category 1: $\Lambda(\eta) = 5\sin(0.25\eta)$

We set $k_5 = 40$, $k_3 = \frac{-260}{3}$, $k_2 = -200$, and $k_1 = -3$. Under these conditions, the maximum Lyapunov exponent (LLE) plots for parameters a, b, c, and d, along with the corresponding two-dimensional and three-dimensional phase diagrams, are shown in Fig. 8. The LLE serves as a key indicator for quantifying the dynamical behaviors of a system, measuring the sensitivity of trajectories to initial conditions [38, 39]. A positive LLE indicates the presence of chaotic behaviors within the system [40]. For parameter a, the LLE values exhibit a fluctuating upward trend, peaking at approximately 1.4×10^{-3}. For parameter b, the LLE values cluster around the 10^{-5} magnitude, markedly smaller than those for parameter a. For parameter c, the LLE curve rises gradually from 0, exhibiting significant fluctuations, with a peak value of 0.18. The behavior of parameter d is broadly similar to that of parameter a. Comparing these perturbation magnitudes, parameter c exhibits the highest overall LLE, indicating its most pronounced influence on the system [41]. The emergence of intersecting trajectories in the two-dimensional phase diagram shown in Fig. 8 (e) and the three-dimensional phase diagram shown in Fig. 8 (f) further corroborates the presence of chaotic phenomena.

Category 2:$\Lambda(\eta) = 5.3\frac{1}{\sqrt{2\pi}}\,\mathrm{e}^{\frac{-(0.03\eta)^2}{2}}$

We set $k_5 = 0.92$, $k_3 = -20$, $k_2 = 11$, and $k_1 = 0.02$. Under this set, the relationship between the LLE and the parameters is illustrated in Fig. 9 (a)–(d). It can be observed that the LLE values are all above 0, indicating the presence of perturbation phenomena. The corresponding two-dimensional and three-dimensional phase diagrams are shown in Fig. 9 (e) and Fig. 9 (f), respectively. The discussion under the Gaussian perturbation term is similar to the previous cases and is therefore not elaborated upon here.

In this section, our research shows that while the original corresponding traveling wave system for EKE has no chaotic behaviors, the corresponding perturbed system shows chaotic behaviors when given appropriate external perturbations, which has been shown through the LLE, two- and three-dimensional phase diagrams. Moreover, the chaotic behaviors shown by the system differ under different perturbation terms. In the current study, we have shown chaotic behaviors only through LLE and phase diagrams. Future work will try to further carry out a theoretical analysis of the chaotic evolution mechanisms within the EKE system.

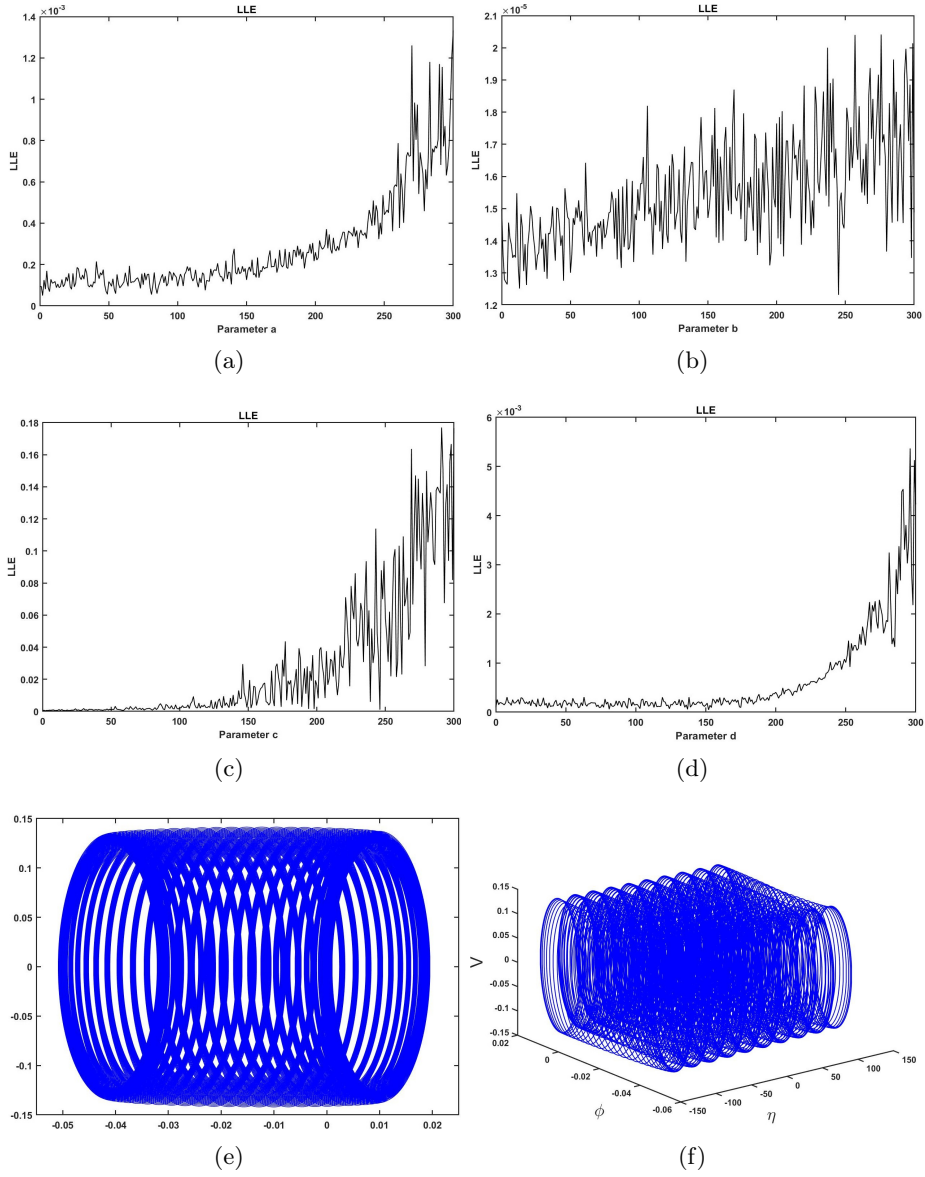

Fig. 8. (a) The LLE of parameter a; (b) The LLE of parameter b; (c) The LLE of parameter c; (d) The LLE of parameter d; (e) The two-dimensional phase diagram of the perturbed system with a sinusoidal function; (f) The three-dimensional phase diagram of the perturbed system with a sinusoidal function.

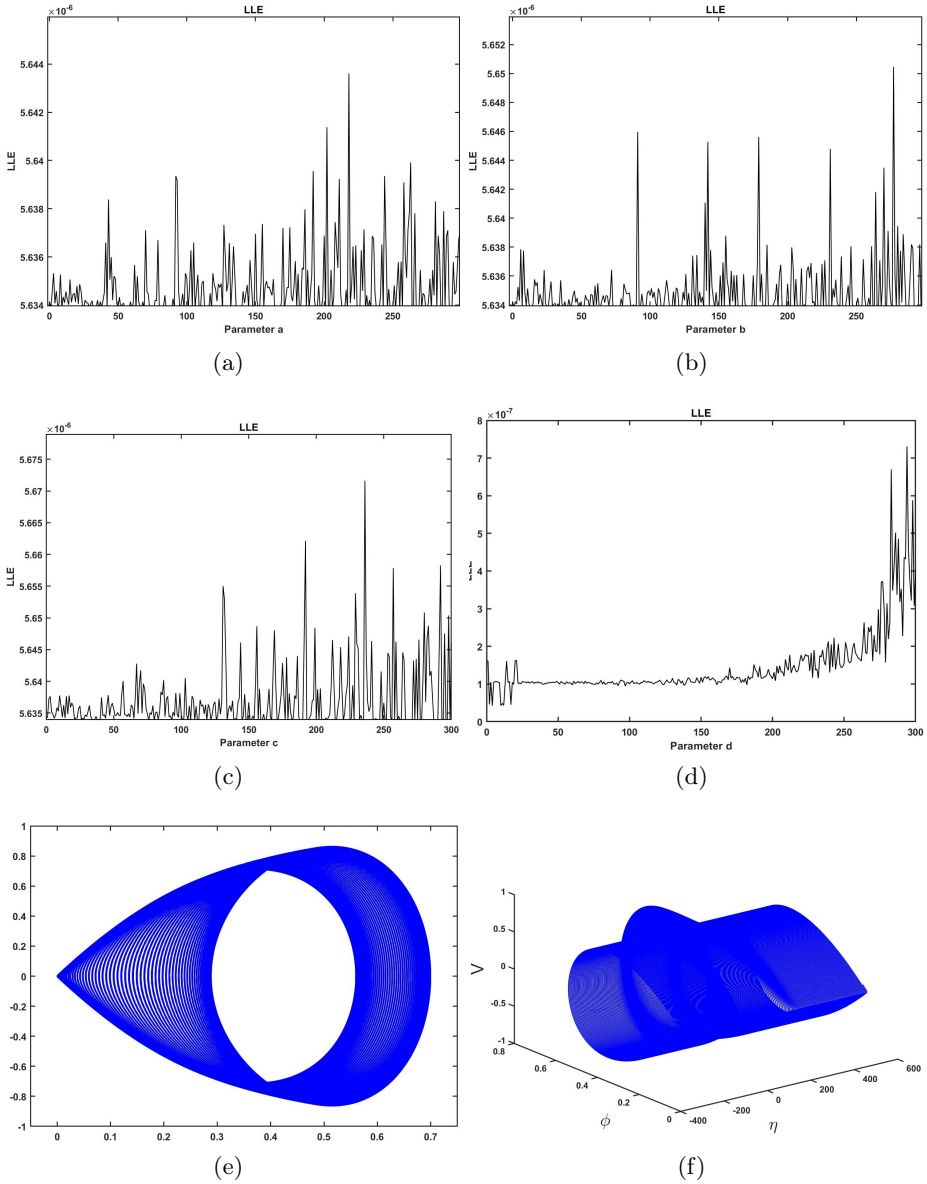

Fig. 9. (a) The LLE of parameter a; (b) The LLE of parameter b; (c) The LLE of parameter c; (d) The LLE of parameter d; (e) The two-dimensional phase diagram of the perturbed system with the Gaussian function; (f) The three-dimensional phase diagram of the perturbed system with the Gaussian function.

6. Conclusion

This paper conducts an in-depth analysis of the EKE equation. First, the EKE equation is simplified into a traveling wave system using the traveling wave transformation. Employing the generalized trial method, we obtain its Gaussian soliton solution for the first time, thereby enriching the solution set of the EKE. Subsequently, we construct the Hamiltonian and plot the phase diagram. Based on bifurcation theory and the derived phase diagram, we have analyzed the dynamical properties of the system, providing a qualitative proof for the existence of soliton and periodic solutions. To verify these qualitative conclusions, we have solved all traveling wave solutions of the EKE. This not only confirms the existence of periodic and soliton solutions but also yields the hyper-elliptic function solution for the EKE for the first time. Such solutions are typically challenging to obtain through conventional methods, highlighting the significance of CDSPM in this research. Finally, we have constructed a perturbed system of the EKE by introducing special forms of the sinusoidal and Gaussian perturbations. The existence of chaotic behaviors is confirmed using the LLE, two-, and three-dimensional phase diagrams, providing new perspectives and methodological foundations for further investigations into the chaotic dynamics of the EKE.

REFERENCES

[1] A. Khan *et al.*, «Investigating the stochastic higher dimensional nonlinear Schrödinger equation to telecommunication engineering», *Sci. Rep.* **15**, 27309 (2025).

[2] A.M. Sultan *et al.*, «Soliton solutions of higher order dispersive cubic-quintic nonlinear Schrödinger equation and its applications», *Chin. J. Phys.* **67**, 405 (2020).

[3] K.K.K. Tam, T.J. Alexander, A. Blanco-Redondo, C.M. de Sterke, «Generalized dispersion Kerr solitons», *Phys. Rev. A* **101**, 043822 (2020).

[4] K.B. Dysthe, «Note on a modification to the nonlinear Schrödinger equation for application to deep water waves», *Proc. R. Soc. Lond. A. Math. Phys. Sci.* **369**, 105 (1979).

[5] S. Theodorakis, «Piecewise linear emulator of the nonlinear Schrödinger equation and the resulting analytic solutions for Bose–Einstein condensates», *Phys. Rev. E* **67**, 066701 (2003).

[6] L. Wang, L. Li, F. Yu, «Some anomalous exact solutions for the four-component coupled nonlinear Schrödinger equations on complex wave backgrounds», *Sci. Rep.* **12**, 16365 (2022).

[7] X. Antoine, W. Bao, C. Besse, «Computational methods for the dynamics of the nonlinear Schrödinger/Gross–Pitaevskii equations», *Comput. Phys. Commun.* **184**, 2621 (2013).

[8] A. Chabchoub *et al.*, «The nonlinear Schrödinger equation and the propagation of weakly nonlinear waves in optical fibers and on the water surface», *Ann. Phys.* **361**, 490 (2015).

[9] L. Ling, L.C. Zhao, B. Guo, «Darboux transformation and classification of solution for mixed coupled nonlinear Schrödinger equations», *Commun. Nonlinear Sci. Numer. Simul.* **32**, 285 (2016).

[10] Y. Yıldırım *et al.*, «Lie symmetry analysis and exact solutions to N-coupled non-linear Schrödinger's equations with kerr and parabolic law nonlinearities», *Rom. J. Phys.* **63**, 103 (2018).

[11] N. Akhmediev, A. Ankiewicz, J.M. Soto-Crespo, «Rogue waves and rational solutions of the nonlinear Schrödinger equation», *Phys. Rev. E* **80**, 026601 (2009).

[12] A.D. Polyanin, N.A. Kudryashov, «Exact solutions and reductions of nonlinear Schrödinger equations with delay», *J. Comput. Appl. Math.* **462**, 116477 (2025).

[13] N.A. Kudryashov, S.F. Lavrova, «Painlevé analysis of the traveling wave reduction of the third-order derivative nonlinear Schrödinger equation», *Mathematics* **12**, 1632 (2024).

[14] E.M.E. Zayed, M.E.M. Alngar, «Optical soliton solutions for the generalized Kudryashov equation of propagation pulse in optical fiber with power nonlinearities by three integration algorithms», *Math. Meth. Appl. Sci.* **44**, 315 (2021).

[15] M. Gu *et al.*, «Explicit solutions of the generalized Kudryashov's equation with truncated M-fractional derivative», *Sci. Rep.* **14**, 21714 (2024).

[16] E.M.E. Zayed *et al.*, «Investigating the generalized Kudryashov's equation in magneto-optic waveguide through the use of a couple integration techniques», *J. Opt.* **54**, 2156 (2025).

[17] M. Sadaf, G. Akram, S. Arshed, H. Sabir , «Optical solitons and other solitary wave solutions of (1+1)-dimensional Kudryashov's equation with generalized anti-cubic nonlinearity», *Opt. Quant. Electron.* **55**, 529 (2023).

[18] X. Hu, Z. Yin, «A study of the pulse propagation with a generalized Kudryashov equation», *Chaos, Solitons Fractals* **161**, 112379 (2022).

[19] M. Mirzazadeh *et al.*, «Dynamics of optical solitons in the extended (3+1)-dimensional nonlinear conformable Kudryashov equation with generalized anti-cubic nonlinearity», *Math. Meth. Appl. Sci.* **47**, 5355 (2024).

[20] H. Ur Rehman *et al.*, «Optical solitons of new extended (3+1)-dimensional nonlinear Kudryashov's equation via ϕ^6-model expansion method», *Opt. Quant. Electron.* **56**, 279 (2024).

[21] W.B. Rabie *et al.*, «Generating optical solitons in the extended (3+1)-dimensional nonlinear Kudryashov's equation using the extended F-expansion method», *Opt. Quant. Electron.* **56**, 894 (2024).

[22] W.B. Rabie *et al.*, «Retrieval solitons and other wave solutions to Kudryashov's equation with generalized anti-cubic nonlinearity and local fractional derivative using an efficient technique», *J. Opt.* **54**, 1992 (2025).

[23] D. Cao, «The classification of the single traveling wave solutions to the time-fraction Gardner equation», *Chin. J. Phys.* **59**, 379 (2019).

[24] D. Cao, C. Li, F. He, «Exact solutions to the space-time fraction Whitham–Broer–Kaup equation», *Mod. Phys. Lett. B* **34**, 2050178 (2020).

[25] X. Yang, «Exact solutions of Wu–Zhang equation via complete discrimination system for polynomial method», *Mod. Phys. Lett. A* **38**, 2350087 (2023).

[26] T. Sarkar, S. Raut, P.C. Mali, «The Classification of the Exact Single Travelling Wave Solutions to the Constant Coefficient KP-mKP Equation Employing Complete Discrimination System for Polynomial Method», *Comput. Math. Methods* **2022**, 3844031 (2022).

[27] L. Jia, L. Tang, «The Classification of Traveling Wave Solutions to Space-Time Fractional Resonance Nonlinear Schrödinger Type Equation with a Special Kind of Fractional Derivative», *Advances in Mathematical Physics* **2021**, 1256745 (2021).

[28] Y. Kai *et al.*, «Qualitative and quantitative analysis of nonlinear dynamics by the complete discrimination system for polynomial method», *Chaos, Solitons Fractals* **141**, 110314 (2020).

[29] Y. Li, Y. Kai Y., «Wave structures and the chaotic behaviors of the cubic-quartic nonlinear Schrödinger equation for parabolic law in birefringent fibers», *Nonlinear Dyn.* **111**, 8701 (2023).

[30] Y. Kai, J. Ji, Z. Yin, «Exact solutions and dynamic properties of Ito-type coupled nonlinear wave equations», *Phys. Lett. A* **421**, 127780 (2022).

[31] Y. He, Y. Kai, «Wave structures, modulation instability analysis and chaotic behaviors to Kudryashov's equation with third-order dispersion», *Nonlinear Dyn.* **112**, 10355 (2024).

[32] J. Li, Z.J. Yang, S.M. Zhang, «Periodic collision theory of multiple cosine-Hermite-Gaussian solitons in Schrödinger equation with nonlocal nonlinearity», *Appl. Math. Lett.* **140**, 108588 (2023).

[33] Y. Gurefe, E. Misirli, A. Sonmezoglu, M. Ekici, «Extended trial equation method to generalized nonlinear partial differential equations», *Appl. Math. Comput.* **219**, 5253 (2013).

[34] K.W. Chow, T.W. Ng, «Periodic solutions of a derivative nonlinear Schrödinger equation: elliptic integrals of the third kind», *J. Comput. Appl. Math.* **235**, 3825 (2011).

[35] A.U. Nielsen *et al.*, «Nonlinear localization of dissipative modulation instability», *Phys. Rev. Lett.* **127**, 123901 (2021).

[36] J.M. Dudley, G. Genty, S. Coen, «Supercontinuum generation in photonic crystal fiber», *Rev. Mod. Phys.* **78**, 1135 (2006).

[37] M.A. Miri, A. Alu, «Exceptional points in optics and photonics», *Science* **363**, eaar7709 (2019).

[38] A. Wolf, J.B. Swift, H.L. Swinney, J.A. Vastano, «Determining Lyapunov exponents from a time series», *Physica D* **16**, 285 (1985).

[39] M.T. Rosenstein, J.J. Collins, C.J. De Luca, «A practical method for calculating largest Lyapunov exponents from small data sets», *Physica D* **65**, 117 (1993).

[40] J.D. Farmer, J.J. Sidorowich, «Predicting chaotic time series», *Phys. Rev. Lett.* **59**, 845 (1987).

[41] M. Balcerzak, D. Pikunov, A. Dabrowski, «The fastest, simplified method of Lyapunov exponents spectrum estimation for continuous-time dynamical systems», *Nonlinear Dyn.* **94**, 3053 (2018).